Journal of Magnetism and Magnetic Materials 471 (2019) 340–345

Contents lists available at ScienceDirect

Journal of Magnetism and Magnetic Materials

journal homepage: www.elsevier.com/locate/jmmm

Research articles

Excitation frequency dependence of temperature resolution in magnetic nanoparticle temperature imaging with a scanning magnetic particle spectrometer

Jing Zhong*, Meinhard Schilling, Frank Ludwig

Institut für Elektrische Messtechnik und Grundlagen der Elektrotechnik, TU Braunschweig, Braunschweig, Germany

ARTICLE INFO

Keywords:
Magnetic nanoparticle temperature imaging
Temperature resolution
Excitation frequency
Signal-to-noise ratio
Temperature sensitivity

ABSTRACT

This paper investigates the dependence of temperature resolution in magnetic nanoparticle (MNP) temperature imaging on the frequency of an applied ac magnetic field with a custom-built scanning magnetic particle spectrometer (SMPS). The fundamental f_0 and $3f_0$ harmonics are measured with the SMPS while the amplitude ratio of the $3f_0$ to f_0 harmonics is used to determine the spatial distribution of temperatures. Experiments on a three-line phantom filled with a MNP sample are performed in different-frequency ac magnetic fields with a constant strength of 8 mT. The standard deviation of measured temperatures is used to characterize the temperature resolution. Experimental results show that the temperature resolution improves from 0.9 K to 0.2 K with increasing the excitation frequency from 600 Hz to 5 kHz, which is mainly caused by a higher signal-to-noise ratio due to Faraday's law and by a higher temperature sensitivity of the $3f_0$ to f_0 harmonic ratio.

1. Introduction

Non-invasive and *in-vivo* temperature imaging is of great significance and interest to biomedical applications, such as magnetic hyperthermia for cancer treatment [1,2] and thermally-controlled drug delivery [3,4]. Magnetic nanoparticle (MNP) thermometry employs the temperature sensitivity of the induced magnetization in ac and/or dc magnetic field for temperature determination [5–8]. For instance, MNP spectroscopy induced in an ac magnetic field has been reported to determine the integral and average temperature of a MNP sample [7–10]. Generally, two harmonics, e.g. the fundamental f_0 and $3f_0$ harmonics, or the $3f_0$ and $5f_0$ harmonics, were measured to determine temperature independent of the MNP concentration [7,9,10]. MNP thermometry is a remote, non-invasive and robust method of temperature determination, which has great potential for in-vivo temperature determination with applications in biomedicine.

To date, multi-dimensional temperature imaging with MNPs is still challenging. Magnetic particle imaging (MPI) has shown great promise in the determination of the spatial distribution of MNP concentration [11–13] while the color-MPI approach has been reported to demonstrate the feasibility of temperature imaging [14]. However, the temperature dependent MNP properties in a gradient and a homogeneous magnetic field have not yet well investigated, as well as the temperature imaging with the MPI approach. Recently, a custom-built scanning magnetic particle spectrometer (SMPS) was built to measure the spatial distributions of magnetic nanoparticle (MNP) harmonics for temperature imaging, extending MNP thermometry from 0-dimensional to 2-dimensional temperature imaging [15]. The spatial distribution of the amplitude ratio of the $3f_0$ harmonic to fundamental f_0 harmonic, which is independent of MNP concentration but dependent on MNP temperature, is used to determine temperature image. In principle, the approach for temperature imaging with the SMPS does not have any depth limitation due to the penetration of magnetic fields, which is an intrinsic advantage compared to optical approaches, such as thermal camera. Thus, the approach can be used for *in-vivo* temperature imaging for some disease diagnostics and therapy, such as breast cancer. However, the spatial resolution is limited by the depth, meaning that a larger depth allows for a worse spatial resolution. In addition, a large depth decreases the strength of the magnetic signal of the MNPs measured by a detection system, which will worsen the resolution of the temperature resolution as well. To compensate the decrease in the magnetic signal strength, a high-frequency ac magnetic field can be used for the excitation of the MNPs. While the temperature dependent MNP magnetic response in static or low-frequency ac magnetic fields can be described by the static Langevin function, in an ac magnetic field with a sufficiently high frequency, MNP relaxation significantly affects the MNP harmonics, as well as temperature sensitivity and resolution. Therefore, the excitation frequency of the applied ac magnetic field is a

* Corresponding author.
E-mail address: j.zhong@tu-braunschweig.de (J. Zhong).

https://doi.org/10.1016/j.jmmm.2018.09.112
Received 18 June 2018; Received in revised form 21 September 2018; Accepted 28 September 2018
Available online 29 September 2018

key influence factor affecting the temperature sensitivity and resolution of the MNP thermometry for temperature determination and imaging. Study on the dependence of the temperature resolution on the excitation frequency is of great interest and significance to improve the temperature resolution.

This paper investigates the temperature resolution in MNP temperature imaging in different-frequency ac magnetic fields with a custom-built SMPS. Specifically, the dependence of the temperature resolution on the excitation frequency, as well as the underlying mechanism, is studied. The standard deviation of the measured temperatures with the 3rd to 1st harmonic ratio, defining the ith harmonic at $i{\cdot}f_0$ frequency, is used to characterize the temperature resolution. Experiments on a three-line phantom are performed at different-frequency ac magnetic fields with constant amplitude of 8 mT. Experimental results of temperature resolution in different-frequency ac magnetic fields are presented. In addition, the underlying mechanisms – The excitation frequency dependence of temperature resolution, including the signal-to-noise ratio (SNR) and the temperature sensitivity – Are discussed.

2. Results and discussion

2.1. Experimental description

A three-line phantom with a distance of 3 mm between two adjacent lines is filled with a MNP suspension for phantom experiments. Fig. 1a shows the three-line phantom filled with MNPs while Fig. 1b shows the schematic of the MNP concentration versus y curve. Each line in the phantom has a length of 8 mm, a width of 2 mm and a depth of 1.5 mm. The experimental sample is SHP-30, purchased from Ocean NanoTech. Ltd. Corp. (San Diego, USA), which consists of Fe_3O_4 single-core nanoparticles with an average core diameter of 30 nm, a coating of monolayer oleic acid and monolayer amphilic polymer, and concentration of 5 mg/ml (Fe).

A custom-built SMPS is used to measure the spatial distributions of the 1st and 3rd harmonics of the MNP sample in different-frequency ac magnetic fields. The excitation frequency is varied from 600 Hz to 5 kHz whereas the excitation magnetic field amplitude is kept constant at 8 mT. A Helmholtz coil in the SMPS is used to generate the ac magnetic fields whereas a gradiometric pickup coil is designed to measure the MNP magnetization. The gradiometric pickup coil has a diameter of about 2.5 mm and a length of 3 mm, which can locally measure the MNP magnetization. The pickup coil is placed about 2–3 mm above the MNP sample (the distance in z-direction/the depth), allowing for a spatial resolution of about 2–3 mm. A mechanical scanner moves the MNP sample, which allows the measurements of the spatial distribution of the MNP harmonics. The SMPS moves the sample far away from the pickup coil for blank measurement to allow the

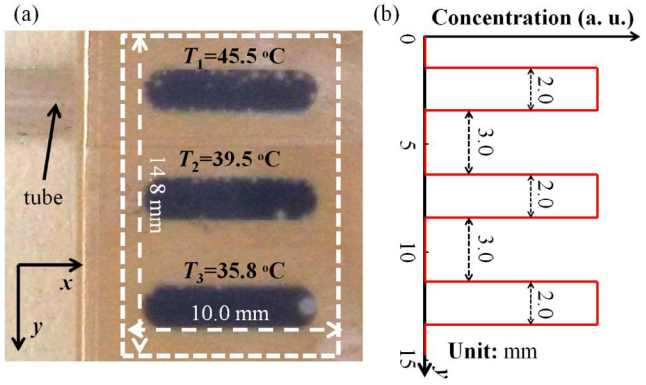

Fig. 1. (a) Photo of the three-line phantom. (b) Schematic of the MNP concentration versus y curve.

measurement of the fundamental harmonic. In the SMPS, the measured ith harmonic amplitude $u_i(x,y)$ can be described by $u_i(x,y) = i\omega{\cdot}s(x,y){*}h_i(x,y)$, where $s(x,y)$ is the point spread function [15,16], defined by the sensitivity profile of the pickup coil, ω is the angular frequency of the excitation magnetic field, $h_i(x,y)$ is the ith harmonic amplitude generated by the local MNPs at a position (x,y). The details of the SMPS design have been presented in [15]. Note that the amplitude of the measured ith harmonic $u_i(x,y)$, in this study, is multiplied with the excitation frequency due to a detection coil based measurement system and the Faraday's law.

A water – Tube with temperature-controlled water, cycled by a pump, is placed under the top-line MNP suspension to heat the MNP sample, as shown in Fig. 1a. The water inside the tube is controlled by a water bath, which allows a stable temperature distribution during the measurements. Thus, the top-line MNP suspension has the highest temperature compared to the other two-line MNP suspensions. A thermal camera was used to measure the temperatures of the centre of the individual line of the phantom, as shown in Fig. 1a. With the same temperature profile of the phantom, the measurements of the MNP harmonics for temperature imaging are performed in different-frequency ac magnetic fields. The scanning field-of-view is 10.0 mm × 14.8 mm in x- and y-direction, respectively.

2.2. Results and discussion

The 1st and 3rd harmonics are measured with the custom-built SMPS for simultaneous imaging of MNP concentration and temperature. Each MNP harmonic is sensitive to MNP concentration and temperature whereas the harmonic ratio, e.g. the 3rd to the 1st harmonic ratio, is independent of MNP concentration but only dependent on MNP temperature. Thus, either the 1st or the 3rd harmonic allows for the measurements of the spatial distribution of MNP concentration whereas the 3rd to 1st harmonic ratio is used to determine the spatial distribution of MNP temperature. During the mechanical scanning of the SMPS, the 1st and 3rd harmonics are measured with a digital lock-in amplifier, realized in LabVIEW, in different-frequency ac magnetic fields.

Fig. 2a and b show the spatial distributions of the measured 1st and the 3rd harmonics at a 2004 Hz ac magnetic field, respectively. Both of the images of the 1st and 3rd harmonics show three blurred lines, corresponding to the experimental phantom in Fig. 1a. It indicates that either harmonic image can be used for MNP concentration imaging. Fig. 2c shows the 1st (left axis) and 3rd (right axis) harmonics versus y curve located at the red dashed lines in Fig. 2a and b whereas Fig. 2d shows the corresponding harmonic ratio M_3/M_1 versus y curve. Note that temperature imaging with a SMPS can only be realized at a specific position where there are enough MNPs. Thus, a threshold δ is applied on $M_1(x,y)$ for the measurements of 2D temperature distribution. At a specific position where $M_1(x,y) < \delta \cdot M_{1,\max}(x,y)$, the harmonic ratio is set to be 0.208 (measured at room temperature = 296 K) while at the specific position where $M_1(x,y) > \delta \cdot M_{1,\max}(x,y)$, the harmonic ratio is calculated from the measured 1st and 3rd harmonics. Herein, δ is set to be 0.75 to avoid any artefacts on the measured temperature at the edge of the line-phantom. $M_{1,\max}(x,y)$ is the maximum value of the 1st harmonic in the whole-image. Fig. 2c shows that the M_3-y curve is slightly different from the M_1-y curve regarding the curve shape, which is caused by the difference in temperature dependent 1st and 3rd harmonics. Fig. 2d shows that the harmonic ratio M_3/M_1 decreases with temperature decreasing due to the heat dissipation by the hot-water tube located at about y = 2.0 mm. This phenomenon is opposite to what is expected from the static Langevin function [7]. The decrease of the harmonic ratio M_3/M_1 with decreasing temperature is caused by the temperature dependent dynamics, i.e., by a faster relaxation at a higher temperature.

The measured temperatures in the centres of the individual lines of the multi-line phantom and the measured harmonic ratio M_3/M_1 are

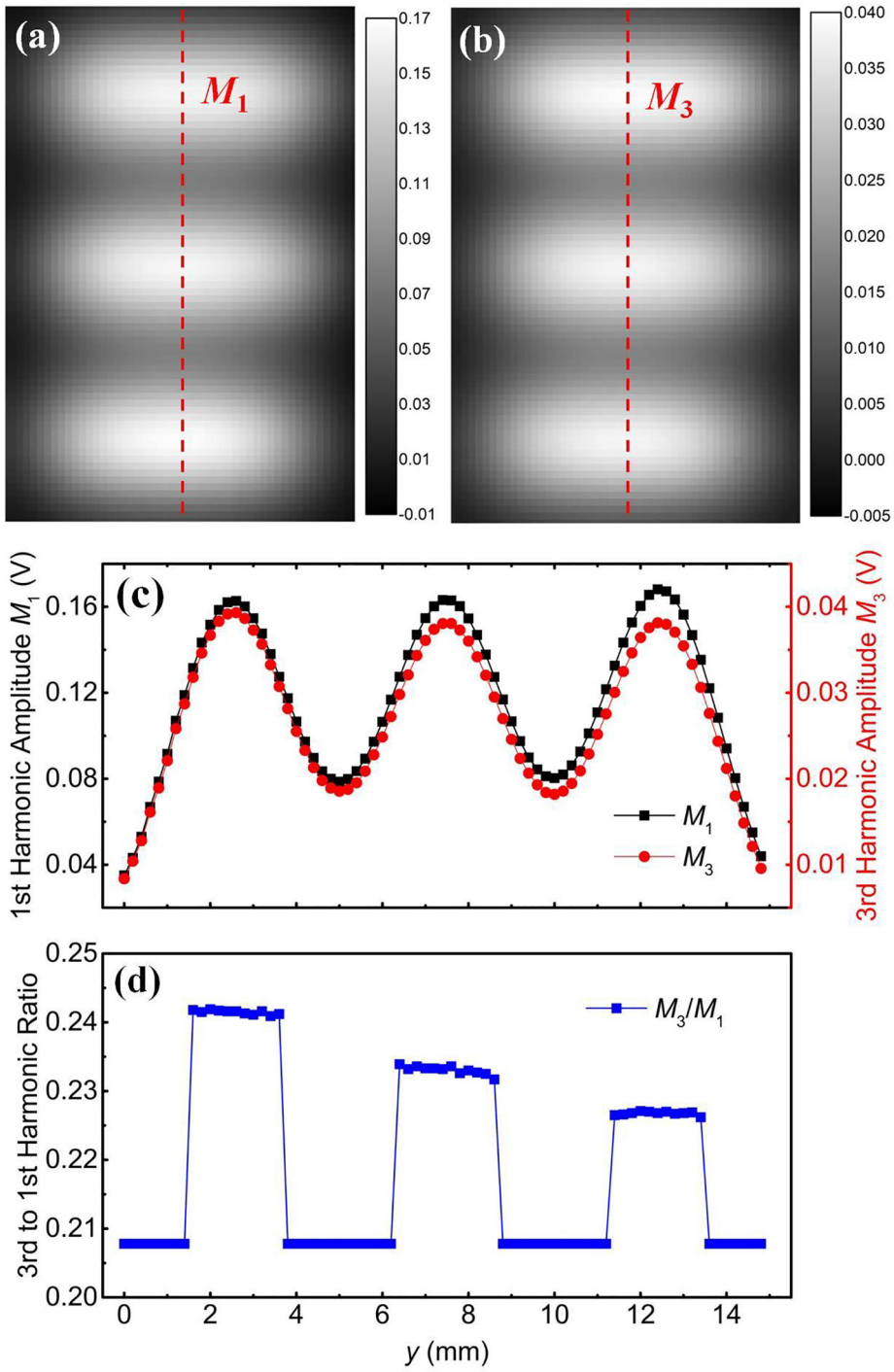

Fig. 2. (a) and (b) show the spatial distributions of the 1st and 3rd harmonics, respectively, at 2004 Hz. (c) shows the 1st (left axis) and 3rd (right axis) harmonic versus y curve located at the red dashed lines in (a) and (b). (d) shows the corresponding harmonic ratio M_3/M_1 versus y curve. Symbols represent the experimental data whereas solid lines in (c) and (d) are a guide to the eye.

used as calibration data of temperature dependent M_3/M_1 to realize temperature imaging, which eliminates systematic errors in the measured temperatures with MNPs. Fig. 3 shows the measured temperature images in ac magnetic fields with frequencies of 615 Hz (a), 1033 Hz (b), 2004 Hz (c), and 5005 Hz (d). All temperature images show that the top lines have the highest temperature and the bottom lines have the lowest temperature, which is in good agreement with the location of the hot-water tube. In addition, the homogeneities in the measured temperature images qualitatively get improved with increasing the excitation frequency. For instance, the bottom line area in Fig. 3a shows the least homogeneous temperatures whereas its homogeneity in Fig. 3d is largely improved.

Fig. 4 shows the corresponding measured 1-dimensional temperature curves of Fig. 3. Fig. 4a depicts the temperature versus y curves located at $x = 5$ mm whereas Fig. 4b shows the temperature versus x curves located at $y = 2.6$ mm, 7.6 mm and 12.6 mm in different-frequency ac magnetic fields. It clearly shows that the measured temperature, as expected, decreases with increasing y. In addition, Fig. 4b shows that the measured temperatures at the same y position, independent of excitation frequency, are the same without taking into

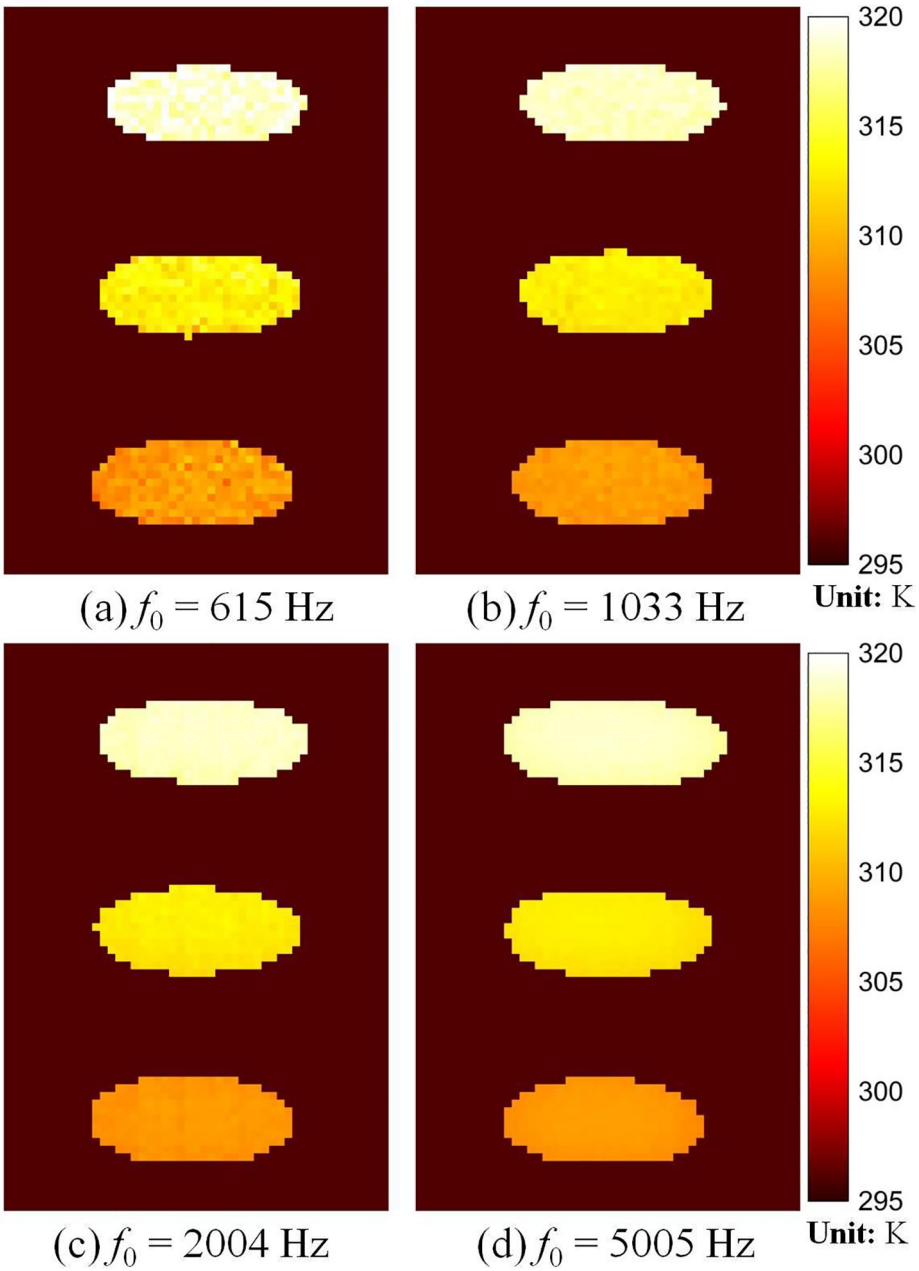

Fig. 3. Temperature images in ac magnetic fields with frequencies of 615 Hz (a), 1033 Hz (b), 2004 Hz (c), and 5005 Hz (d).

account the measurement accuracy. In addition, the fluctuations in the measured temperatures decrease with increasing excitation frequency, as shown in Fig. 4b. It means that the temperature resolution qualitatively improves with an increase in the excitation frequency.

Fig. 5a shows the calculated standard deviation of the measured temperatures at the same y position but different x positions as a function of y. Note that the standard deviation is set to be zero at a specific y position where there are no MNPs for temperature determination. It also shows that the standard deviation decreases with increasing the excitation frequency. The average value of the measured standard deviations at different y positions is used to quantitatively characterize the temperature resolution. Fig. 5b shows the measured temperature resolutions in MNP temperature imaging in different-frequency ac magnetic fields. In 615 Hz ac magnetic field, the temperature resolution is about 0.93 K. With increasing the excitation frequency to 5005 Hz, the temperature resolution improves to about 0.23 K by a factor of about 4. Therefore, in the given frequency range, an increase in the excitation frequency improves the temperature resolution in MNP temperature imaging.

In this paper, MNP temperature imaging is realized by measuring the 1st and 3rd harmonics of a SHP-30 sample. The measured SNRs in dB of both the 1st and 3rd harmonics significantly affect the temperature resolution in the MNP temperature imaging. The SNR and the temperature sensitivity of the harmonic ratio were measured to investigate the underlying mechanism for the excitation frequency dependent temperature resolution. Fig. 6a shows the measured SNRs of the 1st and 3rd harmonics measured on a 35 μl MNP sample with a digital lock-in amplifier method. The noise (MNP harmonic) amplitude is measured via a digital lock-in amplifier without (with) a MNP sample, which allows for the SNR measurement. With increasing the excitation frequency, the SNR of the 1st harmonic gradually increases whereas that of the 3rd harmonic firstly gradually increases and then saturates (slightly decreases). It is caused by frequency multiplication due to Faraday's law and the MNPs' dynamics. According to Faraday's

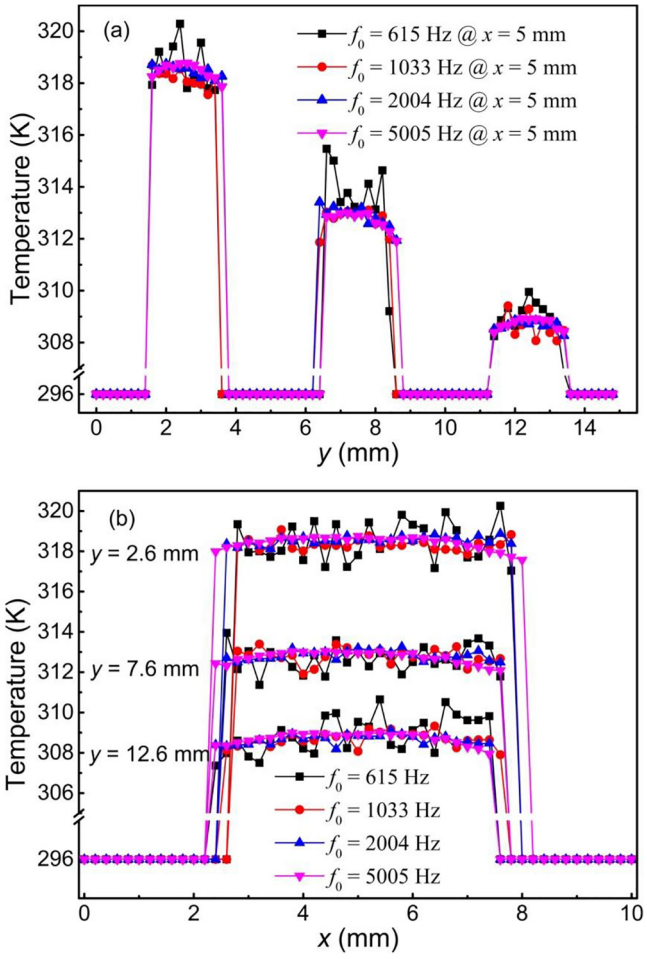

Fig. 4. (a) Measured temperature versus y curve at x = 5 mm in different-frequency ac magnetic fields. (b) Measured temperature versus x curves at different y positions. Symbols represent experimental data whereas solid lines are a guide to the eye.

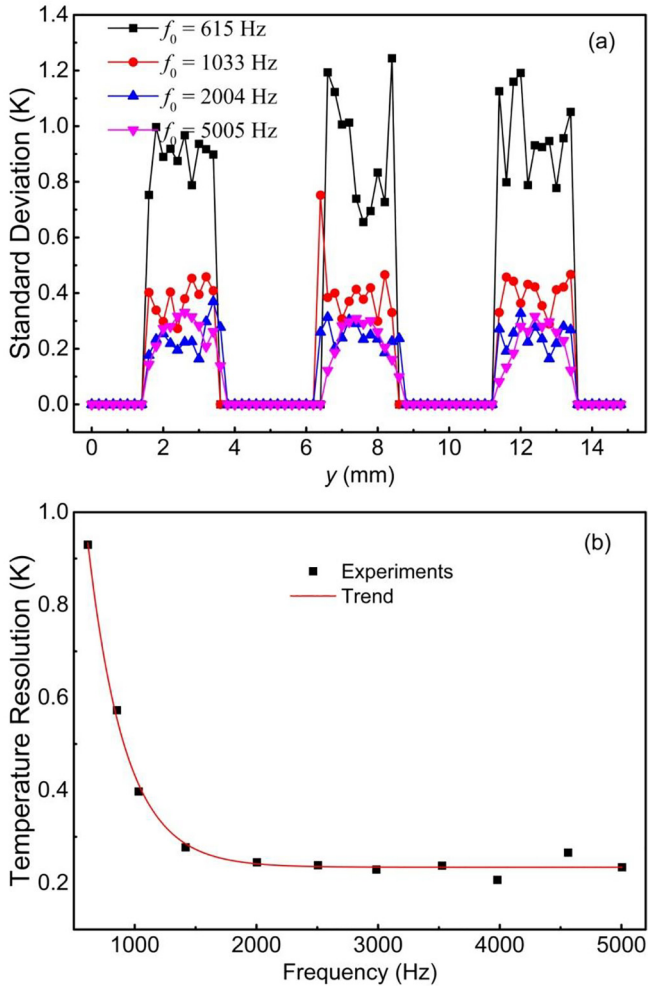

Fig. 5. (a) Calculated standard deviation of the measured temperatures versus y curves in different-frequency ac magnetic fields. (b) Temperature resolution versus excitation frequency. Symbols are experimental results whereas solid line is a guide to the eye.

law, the SNRs of the 1st and 3rd harmonics (multiplied with excitation frequency) in dB measured with a detection coil, in principle, increase linearly with the decadic logarithm of the excitation frequency. However, the MNP dynamics – Brownian relaxation of the experimental MNPs – also significantly affect the signal strength of the MNP magnetization. With a higher excitation frequency, the dynamics of the MNPs decreases the harmonic amplitude of the MNP magnetization. Thus, there is a trade-off between the excitation frequency and the MNP dynamics on the measured harmonic amplitude. For a higher excitation frequency, the strength of the ac magnetization signal increases due to Faraday's law whereas it decreases at higher excitation frequencies due to the finite Brownian relaxation time (the MNPs cannot follow the excitation magnetic field). In addition, a higher harmonic decreases even faster than the fundamental. Thus, the SNR of the 3rd harmonic does not continuously increase but get saturated or even slightly decreases. The magnetization of the experimental MNPs (dominated by Brownian relaxation due to large core size) in this study can be described by Fokker-Planck equation (FPE) with Brownian relaxation. Simulations on the numerical solution of the FPE with Brownian relaxation have been performed to study the frequency dependent harmonic amplitudes, which qualitatively fit with the measurement results very well (simulation results not presented here).

Temperature sensitivity is one of the most important factors significantly affecting the temperature resolution. Fig. 6b shows the measured temperature sensitivities of the 3rd to 1st harmonic ratio at different excitation frequencies. It shows that the temperature sensitivity increases with increasing excitation frequency in the given frequency range. In the FPE, there are two free parameters, ξ(the ratio of the magnetic energy to thermal energy) and $\omega\tau_B$ (ω is the angular frequency of the excitation magnetic field, τ_B is temperature dependent Brownian relaxation time), determining the MNP magnetization behaviour. Due to the Faraday's law, the excitation frequency is one of the key parameters affecting the amplitude of each harmonic with a detection coil based measurement system, as well as the SNR. In addition, both of the parameters ξ and $\omega\tau_B$ are temperature dependent, meaning that the MNP harmonics are temperature sensitive. Due to the influence of the excitation frequency on the SNRs of the 1st and 3rd harmonics and the temperature sensitivity of the 3rd to 1st harmonic ratio, the resulting temperature resolution increases firstly and then saturates with an increase in the excitation frequency. However, one should keep in mind that the highest excitation frequency for the saturated temperature resolution significantly depends on the magnetic properties of the experimental MNPs dominated by Brownian relaxation, e.g. the hydrodynamic size and the medium viscosity.

3. Conclusion

This paper investigates the dependence of the temperature resolution in MNP temperature imaging on the excitation frequency. The 1st and 3rd harmonics of the SHP-30 sample are measured to realize temperature imaging at different-frequency ac magnetic fields with a

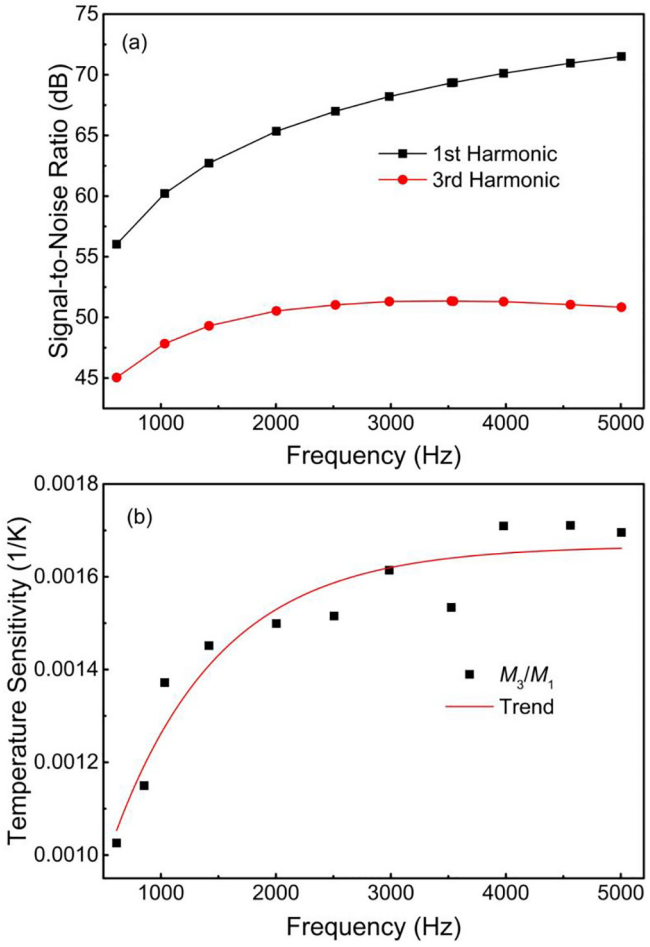

Fig. 6. (a) Measured SNR of the 1st and 3rd harmonics versus frequency curves at room temperature. (b) Measured temperature sensitivity of the 3rd to 1st harmonic ratio versus frequency curve. Symbols represent the experimental results whereas solid curve is a guide to the eye.

constant strength. Experimental results indicate that the temperature resolution increases and then saturates with an increase in the excitation frequency. The signal-to-noise ratios of the 1st and 3rd harmonics, as well as the temperature sensitivity of the 3rd to 1st harmonic ratio, in different-frequency ac magnetic fields are measured and discussed. We emphasize that our experimental findings are of great significance for the improvement of the temperature resolution in MNP thermometry, as well as its biomedical and biological applications.

Acknowledgement

Financial support from Alexander von Humboldt Foundation is acknowledged.

Appendix A. Supplementary data

Supplementary data to this article can be found online at https://doi.org/10.1016/j.jmmm.2018.09.112.

References

[1] Andreas Jordan, Regina Scholz, Peter Wust, Horst Fähling, Roland Felix, Magnetic fluid hyperthermia (MFH): cancer treatment with AC magnetic field induced excitation of biocompatible superparamagnetic nanoparticles, J. Magn. Magn. Mater. 201 (1999) 413–419.
[2] Xu. Ruizhi, Yu. Hui, Yu. Zhang, Ming Ma, Zhongping Chen, Changling Wang, Gaojun Teng, Jun Ma, Xinchen Sun, Gu. Ning, Three-dimensional model for determining inhomogeneous thermal dosage in a liver tumor during arterial embolization hyperthermia incorporating magnetic nanoparticles, IEEE Trans. Magn. 45 (2009) 3085–3091.
[3] Li Li, Timo L.M. ten Hagen, Debby Schipper, Tom M. Wijnberg, Gerard C. van Rhoon, Alexander M.M. Eggermont, Lars H. Lindner, Gerben A. Koning, Triggered content release from optimized stealth thermosensitive liposomes using mild hyperthermia, J. Control. Release 143 (2010) 274–279.
[4] Dirk Schmaljohann, Thermo-and pH-responsive polymers in drug delivery, Adv. Drug Deliv. Rev. 58 (2006) 1655–1670.
[5] Jing Zhong, Wenzhong Liu, Du. Zhongzhou, Paulo C. Morais, Qing Xiang, Qingguo Xie, A noninvasive, remote and precise method for temperature and concentration estimation using magnetic nanoparticles, Nanotechnology 23 (2012) 075703.
[6] Le He, Wenzhong Liu, Qingguo Xie, Shiqiang Pi and P C Morais, A fast and remote magnetonanothermometry for a liquid environment, Meas. Sci. Technol. 27 (2016) 025901.
[7] Ming Zhou, Jing Zhong, Wenzhong Liu, Du. Zhongzhou, Zhixing Huang, Ming Yang, Paulo C. Morais, Study of magnetic nanoparticle spectrum for magnetic nanothermometry, IEEE Trans. Magn. 51 (2015) 6101006.
[8] John B. Weaver, Adam M. Rauwerdink, Eric W. Hansen, Magnetic nanoparticle temperature estimation, Med. Phys. 36 (2009) 1822–1829.
[9] Jing Zhong, Jan Dieckhoff, Meinhard Schilling, Frank Ludwig, Influence of static magnetic field strength on the temperature resolution of a magnetic nanoparticle thermometer, J. Appl. Phys. 120 (2016) 143902.
[10] Jing Zhong, Meinhard Schilling, Frank Ludwig, Magnetic nanoparticle thermometry independent of brownian relaxation, J. Phys. D Appl. Phys. 51 (2018) 9 015001.
[11] Bernhard Gleich, Jürgen Weizenecker, Tomographic imaging using the nonlinear response of magnetic particles, Nature 435 (2005) 1214–1217.
[12] M. Schilling, F. Ludwig, C. Kuhlmann, T. Wawrzik, Magnetic particle imaging scanner with 10-kHz drive-field frequency, Biomedizinische Technik/Biomed. Eng. 58 (2013) 557.
[13] S. Pi, W. Liu, T. Jiang, Real-time and quantitative isotropic spatial resolution susceptibility imaging for magnetic nanoparticles, Meas. Sci. Technol. 29 (2018) 035402.
[14] Christian Stehning, Bernhard Gleich, Jürgen Rahmer, Simultaneous magnetic particle imaging (MPI) and temperature mapping using multi-color MPI, Int. J. Magn. Particle Imag. 2 (2016) 1612001.
[15] Jing Zhong, Meinhard Schilling and Frank Ludwig, Magnetic nanoparticle temperature imaging with a scanning magnetic particle spectrometer, Measurem. Sci. Technol. Submitted.
[16] H. Richter, M. Kettering, F. Wiekhorst, U. Steinhoff, I. Hilger, L. Trahms, Magnetorelaxometry for localization and quantification of magnetic nanoparticles for thermal ablation studies, Phys. Med. Biol. 55 (2010) 623.